



Experimental Investigation of Steel Corrosion in Concrete Structures by Acoustic Emission Analysis

Hisham A. Elfergani ^{1*}

1 Mechanical Engineering Department- Faculty of Engineering- University of Benghazi.

Received: 29 / 03 / 2024; Accepted: 16 / 05 / 2024

ABSTRACT

Corrosion represents a significant issue in various structures, with reinforced and prestressed concrete particularly susceptible. In certain applications, it demands specific attention and mitigation strategies, special attention must be paid to ensure that failure does not occur, as it could lead to loss of life and incur significant financial expenses.

This paper examines the role of Acoustic Emission (AE) as a non-destructive testing (NDT) technique for reinforced concrete structures. The work focuses on the development of experimental techniques and data analysis methods for the detection, location, and assessment of AE from reinforced concrete specimens due to steel wire corrosion.

The results reveal that AE can be used to detect the onset of corrosion activity in wire in the interface between prestressed concrete and mortar as found in prestressed concrete pipes.

It has been shown that by using AE and the relationship between RA and AF value, the crack area can be located and identified. Hence, it could be possible to provide a corrosion alarm and location prior to any wire breaks. Furthermore, the results offer encouragement for the use of the AE technique to detect early corrosion and macro cracks in large concrete pipe structures.

KEYWORDS: Acoustic Emission, Steel Corrosion, reinforced concrete, prestressed concrete.

1. INTRODUCTION

Corrosion of steel is a significant problem in numerous reinforced and prestressed concrete structures. It is reported that the costs of repair and maintenance of corroded structures exceed billions of dollars per year ^[1, 2]. For example, the projected yearly direct expense of corrosion for U.S. highway bridges totals \$13.6 billion, with approximately 40% stemming from corrosion in traditional reinforced concrete (RC).^[3] Infrastructure maintenance and the resulting downtime caused by steel corrosion and its associated issues consume a significant portion of the annual budget allocated for civil structures in numerous countries. The costs vary depending on the condition of the concrete structures, including the cause of damage, degree of damage, and effect of damage on structural behaviour. The risk of corrosion in this particular type of structure requires careful attention as failure could lead to either loss of life in extreme cases or, at the very least, financial losses.

For example, in the collapse of the Polcevera viaduct in Genoa (2018, Italy), which killed 43 people and injured 16, corrosion played a significant role in the collapse, exerting a devastating impact on the inadequately robust design featuring RC stay cables. Additionally, the abrupt collapse of a residential building in Miami (2021, USA), resulting in the loss of 97 lives, was linked to the deterioration of the RC substructure in a marine setting ^[3].

The majority of studies suggest that the primary cause of failure in buildings, bridges, and concrete pipes is corrosion occurring shortly after their construction.

The primary factors leading to the initiation of corrosion in reinforcing and prestressing steel are the infiltration of chloride ions and carbon dioxide onto the steel surface. Once corrosion begins, the resultant corrosion products, typically iron oxides and hydroxides, are commonly deposited within the confined space in the concrete surrounding the steel. Their formation within this confined area generates expansive stresses, leading to cracking and spalling of the concrete cover. Consequently, this process leads to the gradual deterioration of the concrete. ^[4]

Reinforced concrete is recognized as one of the most extensively used building materials. It is relatively cheap, due to the availability of raw materials, versatile,

*Correspondence: Hisham A. Elfergani

Hisham.elfergani@uob.edu.ly

allowing a wide range of forms and applications, and durable if designed and executed in a proper way. The primary factor leading to the degradation of reinforced concrete structures is the corrosion of the steel reinforcement within them.

As a consequence, the expenses associated with repairs constitute a significant portion of current infrastructure spending. Ensuring quality control, maintenance, and planning for the restoration of these structures necessitates non-destructive inspection and monitoring techniques capable of detecting corrosion at an early stage.

The infrastructure of water-carrying concrete pipes has experienced corrosion issues. For instance, the pipes employed in The Man-Made River Project of Libya have experienced this issue. Five instances of pipe failures resulting from corrosion have been documented since their installation. The primary cause of the damage is the corrosion of prestressed wires within the pipes, which occurs due to the penetration of chloride ions from the adjacent soil. Detection of the corrosion in its early stages is very important to avoid water interruption to homes and industries.

The Acoustic Emission (AE) technique has found extensive application in civil engineering for structural health monitoring. Its advantages over other non-destructive techniques include the ability to pinpoint the location of developing cracks and the capability to test the entire structure without disrupting its operation.

Acoustic emission refers to the generation of transient elastic waves resulting from the rapid release of energy from localized sources within a material. AE is generated and propagates during the formation and spreading of cracks in all materials. It can also be defined as the sudden release of elastic waves caused by the rapid energy discharge from localized sources within a material [5]. This abrupt release of elastic energy, known as the AE event, travels through the structure until it reaches the location where a piezoelectric transducer is installed. These transducers identify surface displacement at various points and transform it into a functional electrical signal. Analysing the resulting waveform based on characteristics such as amplitude, energy, and time of arrival enables the evaluation of the severity and origin of the AE source as illustrated in Figure 1.

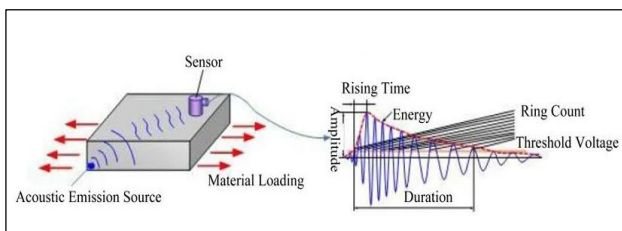


Fig. 1: Acoustic Emission Testing [5].

AE parameters such as amplitude, rise time, average frequency, signal strength, and energy can be further analysed to assess the extent of damage and characterize it. Numerous researchers have devised methodologies for assessing the severity of damage and categorizing cracks using acoustic emission (AE) signal parameters. These methods have used information on the hits, amplitude, frequency, and wave energy [6].

As per multiple studies (references [7, 8, 9, 10, 23, 24, 25]), the connection between RA values (rise time/amplitude) and average frequencies (counts/duration) can serve to categorize different stages of damage in structures. Their findings indicate that a low average frequency and a high RA value in an AE signal denote a shear-type crack, while a high average frequency coupled with a low RA value signifies a tensile-type crack as shown in Figure 2.

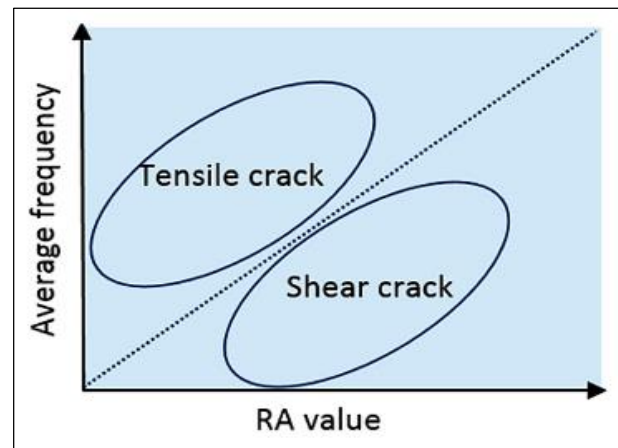


Fig. 2: Crack classification [4]

Concrete pipes used for water transportation are a prime example of structures that have been affected by corrosion. For example, the pipes of The Man-Made River project of Libya have suffered from the effect of corrosion. Five pipe failures have occurred due to corrosion since their installation. This project conveys water through an extensive network of nearly 4000 kilometers of Prestressed Concrete Cylinder Pipe (PCCP) infrastructure [3, 11, 12].

The construction of the concrete pipe involves a 4.0meter diameter, 7.5 meters length and 225 mm thick concrete core encased within a steel cylinder and externally reinforced by prestressed wires. High-tensile steel wires are applied through over-wrapping at a close interval under uniform tension. These prestressed wires are shielded by a 19 mm thick layer of cement mortar. After ten years of operation, there were five severe breakdowns in four-meter-diameter white pipes following a decade of use. The primary cause was the corrosion of the prestressed wires within the pipes, resulting from the assault of chloride ions present in the soil. Early detection of this corrosion is crucial to prevent further pipe failures that could disrupt water flow.

Apart from the ongoing challenge of preventing future corrosion, engineers are actively working to identify the most effective methods for detecting corrosion and halting the deterioration of these pipes [17]. The objective of the Man-Made River project is to employ the Acoustic Emission (AE) method for identifying the initial phases of corrosion before the degradation and ultimate breakdown of concrete structures occur.

While most non-destructive (NDT) methods employed in the project can identify wire breaks, they lack the capability to detect corrosion. Consequently, areas with substantial damage may remain unnoticed in sections where excavation hasn't taken place. In this context, Acoustic Emission (AE) holds a notable advantage over other non-destructive testing methods. It demonstrated the capability of the AE method for detecting the initial stages of the corrosion process, even before significant damage to the concrete occurs. Moreover, it can gauge the extent of damage being inflicted on the concrete [13, 14, 15, 16, 22].

2. EXPERIMENTAL SETUP

• Wire preparation

As the aim of this study was to replicate the authentic physical environment surrounding the high-strength steel wires in concrete pipes, it was crucial to position and sustain all pertinent wire samples under tension equivalent to 60% of their ultimate tensile strength in PCCP. To achieve this objective a tension frame was designed and constructed. The framework comprises two blocks measuring 190mm x 45mm x 45mm each, along with two threaded steel bars (studding) with a diameter of

20 mm and a length of 500 mm. Two holes (20 mm diameter) and two (6mm) are drilled in each block. The two blocks are connected using two threaded bars secured by eight nuts. The two working high-strength steel wire samples were used. The metallurgical composition and mechanical properties of wire are summarized as follows: Carbon steel (carbon 0.8-0.84%, 0.85-1.00%Mn, 0.030 %Max S, 0.035% Max P, 0.20-0.35% Si) [26]. The wires exhibit a tensile strength of approximately 1738 MPa. The two wire samples were passed through 6 mm diameter holes in the steel blocks and then two modified bolts and nuts. Finally, a steel cylinder was threaded over the wire and then was compressed in a load machine. By adjusting the bolts and nuts, each wire was subjected to a tensile force of 20 kN, which was monitored using strain gauges attached to the wires. [16, 17, 20].

• Concrete and mortar preparation

The concrete specimen (200*200*50mm), representative of the inner pipe was prepared according to the technical specification for PCCP manufacturing used in the Man-Made River Project, which is in accordance with AWWA C301-92 (Standard for Pre-stressed Concrete Pressure Pipe, Steel Cylinder Type, for Water and Other Liquids) [3]. Three days following the casting of the concrete specimen, the wires, along with their holding frame, were positioned on the upper surface of this specimen. Finally, the mortar 200*200mm and 20 mm thickness was coated on the upper surface of the concrete. The mortar consists of one part cement to not more than three parts fine aggregate by weight [6, 18, 21]. The final construction is shown in Figure 3.



Fig. 3: Concrete and mortar sample

• Accelerated corrosion technique

In order to examine the impacts of corrosion within a practical timeframe, it may be essential to speed up the beginning phase and at times regulate the corrosion rate as it progresses. To simulate the corrosion of steel wires,

the corrosion cell was induced by an impressed current ($100\mu\text{A}/\text{cm}^2$). This is documented as representing the maximum corrosion rate for concrete under laboratory conditions and has been utilized by numerous researchers in their laboratory experiments, as discussed by Li and Zhang [18]. In this experimental setup, wire corrosion was

induced by applying an impressed current of $100\mu\text{A}/\text{cm}^2$. The prestressed wires were integrated into an electrical circuit with the positive pole of the power supplier, while the negative pole was connected to a stainless-steel plate (30*150 mm) positioned on the upper mortar. A 4% NaCl solution was poured on the surface of the mortar. Silicon sealant was employed to create a pool of the solution on the upper surface.

• *Acoustic emission set-up*

Typically, AE instrumentation comprises transducers, filters, amplifiers, and analysis software. Four AE sensors (R3I – resonant frequency is 30 kHz) were mounted to the surface of the mortar as shown in Figure4. The four AE sensors were affixed using silicon sealant and secured onto the upper surface of the mortar with a U-shaped plate. This plate was screwed in place to firmly hold down the sensors and ensure effective coupling. Then the sensitivity of the sensors was checked by using the Hsu-Neilson source [19]. The Schematic diagram and a photo of experimental test set up are shown in Figures 4 and 5.

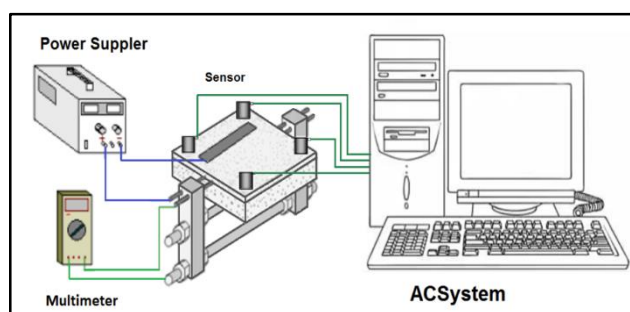


Fig. 4: Detailed schematic view of experimental set-up

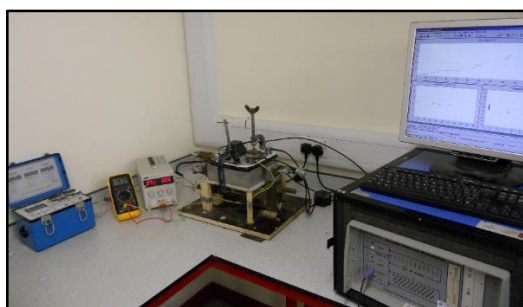


Fig. 5: A Photo of Experimental Set-up

3. RESULTS AND DISCUSSION

Figure 6 depicts a schematic representation of the specimen post-testing, illustrating the placement of sensors on the mortar surface, wire positioning, the stainless-steel plate, and the shape of the crack. Figures 7 display photographic images of the top surface of the mortar after the finish of the test.

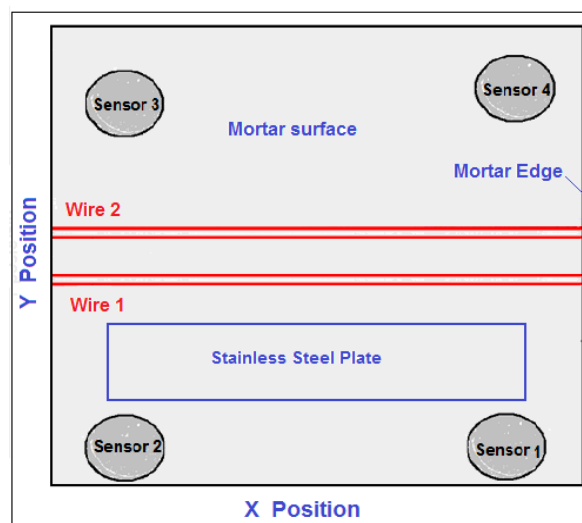


Fig. 6: Schematic Diagram of top mortar surface

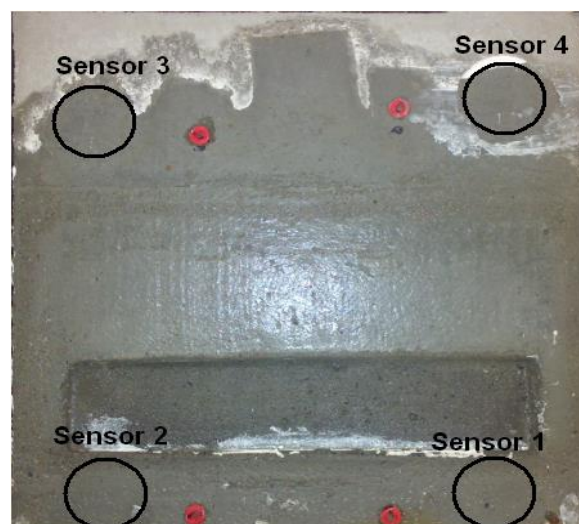


Fig. 7: photo of top mortar surface

Figure 8 shows the cumulative acoustic energy as detected by all sensors with a minimum amplitude 42 dB for almost 100 hr of continuous monitoring. The graph demonstrates the behaviour of the energy emission in two regions of time.

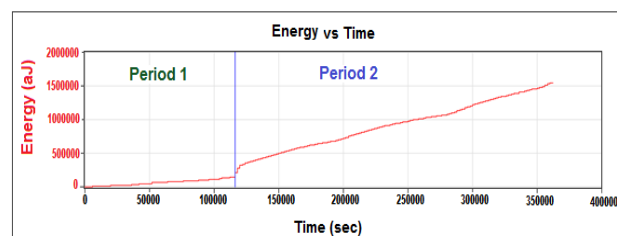


Fig. 8: Energy of detected signals for the duration of the investigation

It can be noted that the whole time of the test can be divided into two significant stages as shown in Figure 8, the first stage which is the first 30 hr (0-120,000 sec) is named period 1. There are a small number of hits and with low energy. The second stage which is 70 hr (120000-370000) is named period 2. It can be noted that there is a sudden increase in the number of hits and higher energy emitted is attributed to the onset of corrosion and the build-up of corrosion products on the corroding wire surface.

Figure 9 shows the source location of the sample of period 1 before supplying current (no corrosion) for about 30 hours. It can be seen that there is a low level of events prior to the onset of corrosion. Additionally, a color-coded legend is provided to indicate the number of signals detected at each position.

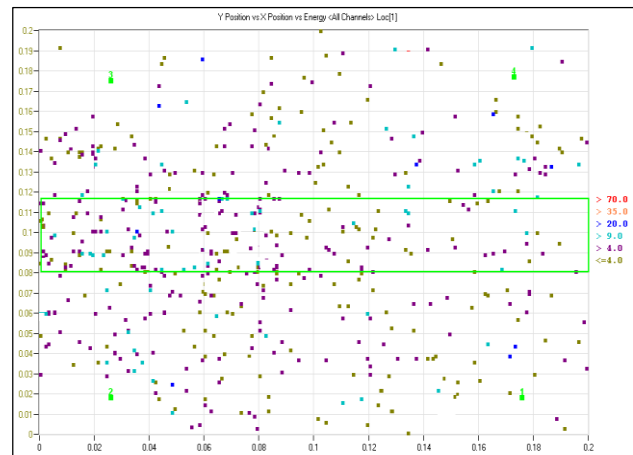


Fig. 9: Source locations before supplying current (no corrosion)

Figure 10 (a) illustrates the trends of the relation between the RA-value and AF-value of all hits for period 1 of concentration of events on the surface of the mortar. Furthermore, these areas can be visualised by using Kernel Density Estimation Function (KDEF) as shown in Figure 10 (b). Areas with high concentrations are more readily identifiable. The concentration value of the data is represented by different colours, brown for the highest number of data points and blue for the lowest. It can be noted that the RA vs AF relationship has a broad horizontal distribution (0-20 ms/v) which is representative of non-corrosion signals.

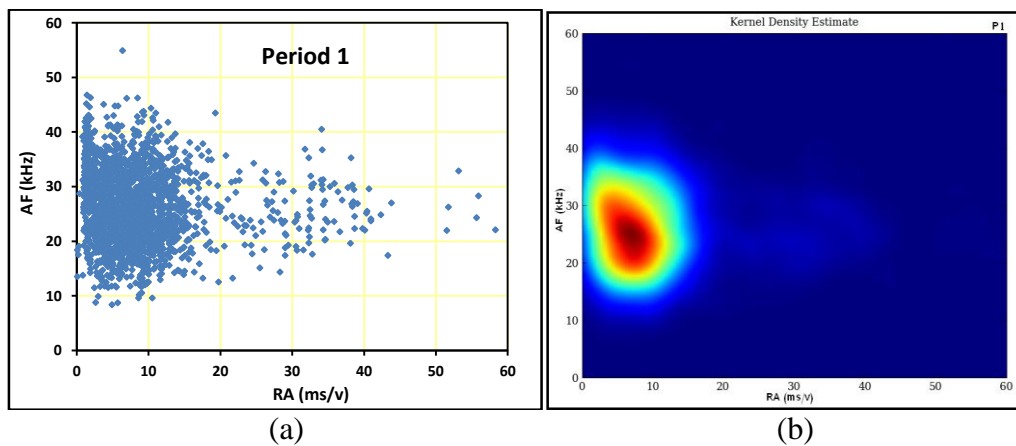


Fig. 10: Relation between the RA value and AF, (a) graph and (b) Kernel Density Estimation Function

Figure 11 illustrates the source locations of signals during this period 2. It can be noted that the highest hits concentration and highest energy in the region coincides with the maximum wire corrosion products area which was visibly observed post-test as shown in Figure 12.

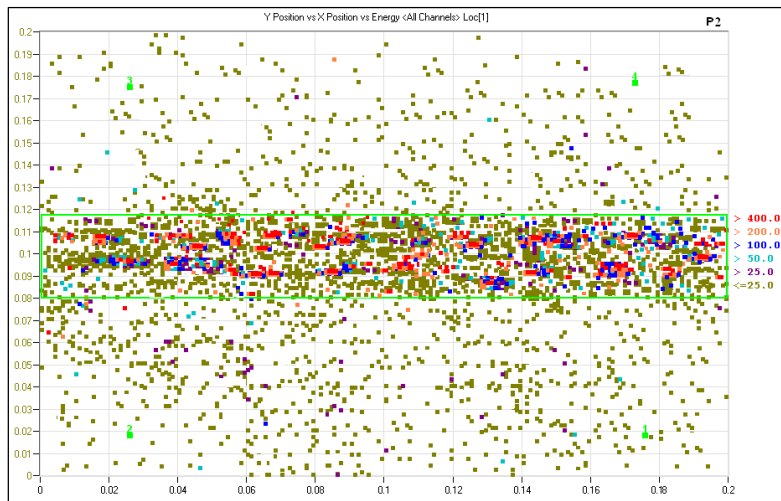


Fig. 11: Source locations for period 2

Figure 12 displays the corroded wires and corrosion products after the mortar has been removed. It is evident that significant corrosion occurred in the upper where a vast majority of AE signals were detected and pinpointed.

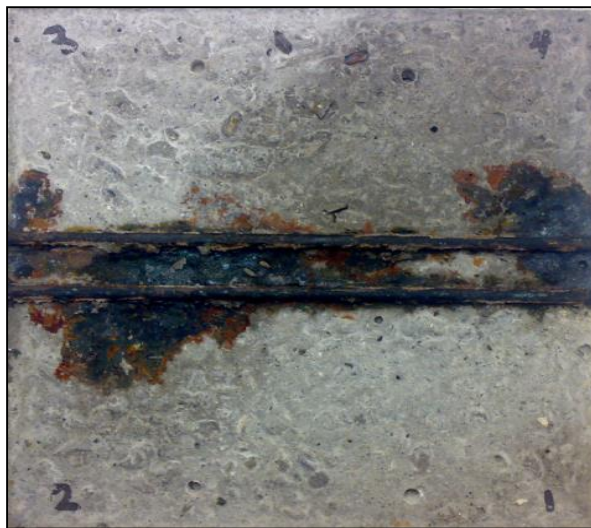


Fig. 12: Photo of the upper concrete surface and corroded wires

Figure 13 illustrates the trends of relation between the RA-value and AF-value of all hits of the period, which are represented via graph and KDEF. It can be seen that the most of data points have various AF values and low RA values (less than 10 ms/v) which are termed a “vertical trend”, this indicates the wire corrosion activity.

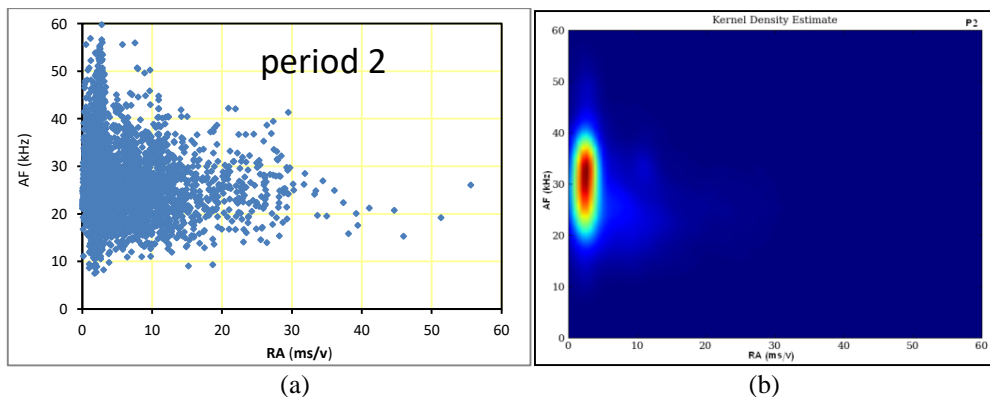


Fig. 13: Relation between the RA value and AF, (a) graph and (b) Kernel Density Estimation Function of period 2

It has been shown that by using AE and the relationship between RA and AF value, the corrosion area can be located and identified (Figures 11 and 12). Hence, it could be possible to provide a corrosion alarm and location to pipe engineers prior to any wire breaks. Furthermore, it is possible to identify the corrosion activity area before the mortar fails to appear.

4. CONCLUSION

The results demonstrated that the acoustic emission method is an excellent non-destructive method to monitor the different stages of deterioration of concrete structure. It was shown that the AE method is sensitive to detect the stages of steel corrosion prior to the deterioration of reinforced concrete structures. In addition, it can identify the onset of corrosion activity by analysing AE signal parameters and the relationship between RA value and AF value. It was shown that using AE it is possible to give indications of damage at earlier stages than traditional techniques. Furthermore, the results offer encouragement for the use of the AE technique to detect early corrosion and macro cracks in large concrete pipe structures.

5. REFERENCES

- Ann K.Y., Ahn J. H., Ryou J. S. (2009). The importance of chloride content at the concrete surface in assessing the time to corrosion of steel in concrete structures, *Construction and Building Materials*, 23, pp239–245.
<https://doi.org/10.1016/j.conbuildmat.2007.12.014>
- Zhe L., Zuquan J., Penggang W., Tiejun Z. (2021) Corrosion mechanism of reinforced bars inside concrete and relevant monitoring or detection apparatus: A review, *Construction and Building Materials Journal* Vol. 279, 12 April, pp 122432.
<https://doi.org/10.1016/j.conbuildmat.2021.122432>
- Verstryngne E., Steen C., Vandecruys E., Wevers M. (2022). Steel corrosion damage monitoring in reinforced concrete structures with the acoustic emission technique: A review, *Construction and Building Materials*, Volume 349, 26 September, 128732.
<https://doi.org/10.1016/j.conbuildmat.2022.128732>
- Fujian T., Guoshuai Z., Hong-Nan L., Els V. (2021). A review on fiber optic sensors for rebar corrosion monitoring in RC structures, *Construction and Building Materials Journal*, Vol. 313, 27 December, pp 125578.
<https://doi.org/10.1016/j.conbuildmat.2021.125578>
- Miller R. K., Hill E. V. K., Moore P. O. (2005). *Non-destructive Testing Handbook, Acoustic Emission Testing*, Volume 6, USA.
- Elfergani H. (2024). Acoustic Emission Analysis for Crack Classification and Localization in Prestressed Concrete Structures, *International Science and Technology Journal*, vol. 33, Issue 2, January, pp 1-15.
- JCMS-III B5706. (2003). *Monitoring method for active cracks in concrete by AE*, Tokyo: Japan Construction Material Standards.
- Ohtsu M. and Tomoda Y. (2007). Corrosion process in reinforced concrete identified by acoustic emission, *Materials Transactions*, Vol. 48, No. 6, pp1184-1189.
<https://doi.org/10.2320/matertrans.I-MRA2007844>
- Ohno K. And Ohtsu M. (2010). Crack classification in concrete based on acoustic emission, *Construction and Building Materials* 24, pp 2339-2346.
<https://doi.org/10.1016/j.conbuildmat.2010.05.004>
- Aggelis D. (2011). Classification of cracking mode in concrete by acoustic emission parameters, *Mechanics Research Communications* 38, pp153-157.
<https://doi.org/10.1016/j.mechrescom.2011.03.007>
- Kuwairi A. (2006). Water mining: the Great Man-made River, Libya, *Proceedings of ICE Civil Engineering* 159 May, pp 39-43 paper 14382.
<https://doi.org/10.1680/cien.2006.159.5.39>
- Essamin O. and Holley M. (2004). Great Man Made River Authority (GMRA): The Role of Acoustic Monitoring in the Management of the World Largest Prestressed Concrete Cylinder Pipe Project, *Proceedings of the ASCE Annual International Conference on Pipeline Engineering and Construction*, August 1-4, San Diego, California.
[DOI: 10.1061/40745\(146\)28](https://doi.org/10.1061/40745(146)28)
- Ing M., Austin S., Lyons R. (2005). Cover zone properties influencing acoustic emission due to corrosion, *Cement and Concrete Research* 35 pp 284– 295.
<https://doi.org/10.1016/j.cemconres.2004.05.006>
- Hellier C. J. (2001). *Handbook of Non-destructive Evaluation*, McGraw-Hill, USA.
- Carpinteri A., Lacidogna G., Pugno N. (2007). Structural damage diagnosis and life-time assessment by acoustic emission monitoring. *Engineering Fracture Mechanics* 74, pp273–289.
<https://doi.org/10.1016/j.engfracmech.2006.01.036>
- Elfergani H., Pullin R., Holford K. (2011). Acoustic Emission Analysis of Prestressed Concrete Structures. *Journal of Physics: Conference Series* 305, 012076.
<https://doi.org/10.1088/1742-6596/305/1/012076>
- Elfergani H., Pullin R., Holford K. (2013). Damage assessment of corrosion in prestressed concrete by acoustic emission, *Construction & Building Materials Journal*, Vol. 40, pp 925-933.
<https://doi.org/10.1016/j.conbuildmat.2012.11.071>
- Li X. and Zhang Y. (2008). Analytical Study of piezoelectric Paint for Acoustic Emission-Based Fracture Monitoring, *Fatigue and Fracture of Engineering Materials and Structures* 31, pp. 684-694.
<https://doi.org/10.1111/j.1460-2695.2008.01249.x>

19. Hsu N N, and Breckenridge, F. R. (1981). Characterization and Calibration of Acoustic Emission Sensor. *Materials Evaluation* 39 (1) pp. 60-68.
20. Shahidan S., Pulin R., Bunnori N. M., Holford K. M. (2013). Damage classification in reinforced concrete beam by acoustic emission signal analysis, *Construction and Building Materials*, Vol. 45, August , pp 78-86.
<https://doi.org/10.1016/j.conbuildmat.2013.03.095>
21. Elfergani H. (2024). Monitoring Stages of Damage in Concrete Structures by Using the Acoustic Emission Technique, *African Journal of Advanced Pure and Applied* vol. 3, Issue 1, January – Marc, pp 127-133.
22. Liu F., Guo R., Lin X., Zhang X., Huang S., Yang F., Cheng X. (2022). Monitoring the damage evolution of reinforced concrete during tunnel boring machine hoisting by acoustic emission, *Construction and Building Materials Journal*, Vol. 327, 11 April, pp 127000.
<https://doi.org/10.1016/j.conbuildmat.2022.127000>
23. Lian S., Zheng K., Zhao Y., Bi J., Wang C., Huang Y. (2023). Investigation the effect of freeze–thaw cycle on fracture mode classification in concrete based on acoustic emission parameter analysis, *Construction and Building Materials Journal* Vol. 362, 2 January, pp 129789.
<https://doi.org/10.1016/j.conbuildmat.2022.129789>
24. Yong N., Xiao-Ping Z., Filippo B. (2020). Evaluation of fracture mode classification in flawed red sandstone under uniaxial compression, *Theoretical and Applied Fracture Mechanics Journal*, Vol. 107, June, 102528.
<https://doi.org/10.1016/j.tafmec.2020.102528>
25. Abarkane C., Florez-Tapia A., Odriozola J., Artetxe A., Lekka M., García-Lecina E., Grande H., Vega J. (2023). Acoustic emission as a reliable technique for filiform corrosion monitoring on coated AA7075-T6: Tailored data processing, *Corrosion Science* Vol.214, 15 April,110964.
<https://doi.org/10.1016/j.corsci.2023.110964>
26. ASTM A663/A663M-89. 2000. Specification for Steel Bars, Carbon, Merchant Quality, Mechanical Properties, American Society for Testing and Materials.